LC–MS/MS analysis of twelve neurotransmitters and amino acids in mouse cerebrospinal fluid

María Encarnación Blanco[a,c], Olga Barca Mayo[b], Tiziano Bandiera[c], Davide De Pietri Tonelli[b], Andrea Armirotti[a,d,*]

[a] Graphene Labs, Fondazione Istituto Italiano di Tecnologia, Genova, Italy
[b] Neuro miRNA Lab, Fondazione Istituto Italiano di Tecnologia, Genova, Italy
[c] D3-Pharmachemistry, Fondazione Istituto Italiano di Tecnologia, Genova, Italy
[d] Analytical Chemistry and In-vivo Pharmacology Facility, Fondazione Istituto Italiano di Tecnologia, via Morego 30, 16163 Genova, Italy

ABSTRACT

Background: So far, analytical investigation of neuroactive molecules in cerebrospinal fluid (CSF) of rodent models has been limited to rats, given the intrinsic anatomic difficulties related to mice sampling and the corresponding tiny amounts of CSF obtained. This poses a challenge for the research in neuroscience, where many, if not most, animal models for neuronal disorders rely on mice.
New method: We introduce a new, sensitive and robust LC–MS/MS method to analyze a panel of twelve neuroactive molecules (NM) from mouse CSF (aspartic acid, serine, glycine, glutamate, γ-aminobutyric acid, norepinephrine, epinephrine, acetylcholine, dopamine, serotonin, histamine and its metabolite 1-metylhistamine). The paper describes the sampling procedure that allows the collection of $1-2$ microliters of pure CSF from individual mouse specimens.
Results: To test its applicability, we challenged our method on the field, by sampling 37 individual animals, thus demonstrating its strength and reliability.
Comparison with existing method(s): Compared to other methods, our procedure does not involve any extraction nor derivatization steps: samples are simply diluted and analyzed as such by LC–MS/MS, using a dedicated ion pairing agent in the chromatographic setup. The panel of neuroactive molecules that is analyzed in a single run is also significantly higher compared to other methods.
Conclusions: Given the number of mouse models used in the neuroscience research, we believe that our work will pave new ways to more advanced research in this field.

1. Introduction

Neuroactive molecules (NM) are a class of endogenous molecules released by presynaptic neurons in the synaptic cleft, where they bind to receptors present on the membrane of postsynaptic neurons (Lodish et al., 2000). The continuous release and depletion of NM at synapses represents the mechanism for signal transduction in the brain. The chemical space of NM is huge, ranging from gases like NO (Kuriyama and Ohkuma, 1995), to monoamines (Doummar et al., 2018), to amino acids (Bowery and Smart, 2006), to lipids (Bernabo et al., 2013), to the continuously growing family of neuropeptides (Carr and Frings, 2019). Given their key role in any function of the nervous system, NM quantification represents a cornerstone for many different research fields in

neurology (Sourkes, 2010), developmental biology (Pirola, 1988) and behavioural studies (Karrenbauer et al., 2011) and many others (Rodan et al., 2015; Hyland, 2008). Cerebrospinal fluid (CSF), being continuously in contact with the brain, is the most important biofluid for NM analysis as it gives an immediate readout of their modulation in the central nervous system (CNS). CSF analysis is routinely used in clinical practice (Rodan et al., 2015) and NM have been proposed as biomarkers for many pathological conditions (Temudo et al., 2009), including Parkinson's (de Jong et al., 1984; Gibson et al., 1985) and Alzheimer's diseases (Bruno et al., 1995). Liquid chromatography coupled to tandem mass spectrometry (LC−MS/MS) represents the state-of-the-art tool for an accurate and reliable quantification of NM from CSF (Cox et al., 2015; Han et al., 2018), given its sensitivity, selectivity and

---

linearity in the response over a broad span of analyte concentrations (Jiang et al., 2016; Voehringer et al., 2013). CSF sampling in humans, albeit invasive and unpleasant, is relatively easy to perform and it normally allows the sampling of consistent volumes (up to milliliter scale), thus greatly facilitating the analytical workflow. More complicated is the situation for NM quantification in CSF for animal models. As far as rodents are concerned, CSF analysis is performed in rats, whose anatomy normally allows the sampling of tens, if not hundreds, of microliters of CSF Han et al., 2018; Voehringer et al., 2013), while few studies are performed in mice. The scarcity of studies in mice CSF is a result of the size and anatomy of these animals. It is estimated that mice have around a total of $35-40\,\mu L$ of CSF (Pardridge, 2016; Simon and Iliff, 2016), with even lower volume in young specimens. The collection of CSF from the cisterna magna in mice is a delicate maneuver. Furthermore, due to its closeness to blood vessels, a meticulous surgery is required to avoid sample contamination. This is crucial in NM analysis, as the concentration of NM in blood greatly differ from that of CSF and blood contamination may distort the results obtained in quantitative analyses. Moreover, the area for CSF collection in mice is also difficult to dissect and often only small samples are obtained (around of $5-7\,\mu L$ or less), thus putting the sensitivity of the analytical workflow under great pressure. This implies that several extremely important *mouse* models have so far been out of reach of routine NM quantification in CSF, like, for example, EAE for multiple sclerosis (Dang et al., 2015) or 6-OHDA for Parkinson's (Thiele et al., 2012). The LC−MS analysis of NM in mice CSF is challenging. Monoamine (MANM) and amino acid NM (AANM) are polar, low MW molecules. This type of compounds are notoriously hard to analyze by conventional LC−MS/MS methods, as they show very poor retention, if any, in reversed phase (RP) mode. Some methods have been developed to increase the retention of these compounds by performing diverse chemical derivatization reactions such as benzoylation (Cox et al., 2015), dansylation (Cai et al., 2010), or succinimide based derivatization (Zhang et al., 2014) among others (Bovingdon and Webster, 1994). However, these procedures are usually time consuming and prone to low reproducibility. To improve the retention of NM without derivatization, the use of hydrophilic liquid chromatography (HILIC) has been explored. HILIC is popular in the analysis of polar analytes, and it has been used in the past for several NM (Inoue et al., 2016; Wu et al., 2018). Notwithstanding, in terms of peak shape, equilibration time required, robustness and throughput, RP−LC remains the preferred option. Another approach to improve retention of NM in RP, is the use of volatile ion-pairing reagents. This was the approach adopted by Romero-Gonzalez et al. and Zhu et al. that used heptafluorobutyric acid (HFBA) in the analysis of nine NM and metabolites in rat brain homogenates (Gonzalez et al., 2011) and acetylcholine and choline in rat brain microdyalisates (Zhu et al., 2000), respectively. Making mouse CSF accessible to routine NM evaluation would be highly beneficial for many reasons (costs savings included) and it would thus represent a major breakthrough in brain research. This is the purpose of the present work. We setup and validated a new method for the analysis of 12 polar neuroactive molecules in the CSF of a single, individual mouse. All the selected NM have very well-known and relevant biological roles in CNS physiology (Noriega-Ortega et al., 2011; Ramakrishnan and Namasivayam, 1995; Sustkova-Fiserova et al., 2009): aspartic acid (Asp), serine (Ser), glycine (Gly), glutamate (Glu), γ-aminobutyric acid (GABA), norepinephrine (NE), epinephrine (EP), acetylcholine (ACh), dopamine (DA), serotonin (5-HT), histamine (His) and its metabolite 1-metylhistamine (MHis) (Marsavelski and Vianello, 2017). The method consists of (a) an advanced surgical procedure that allows a reliable sampling of $1-2\,\mu L$ of blood-free CSF from the cisterna magna of the mouse and (b) a new, sensitive LC−MS/MS method that we developed and fully validated. We then tested our method on a group of 37 animals, consisting of male and female mice ranging from 6 to 70 weeks of age.

2. Results and discussion

2.1. CSF sampling

CSF sampling from mice has always been difficult, with the total CSF volume collected strongly depending on the size and strain of the mouse (Liu and Duff, 2008; Sakic, 2019). It was previously reported that adult males provide maximum amounts in the following order: Balb/C < C57 Bl/6 < CD1, SW and MRL (up to $40\,\mu L$) (Sakic, 2019). Two previous studies reported CSF collection from the cisterna magna of C57 Bl/6 mice of the same age used in the present study. In the first one, Fleming and colleagues collected 5–15 µL of CSF by aspiration with a needle-pipette junction attached to a mouth suction apparatus (Fleming et al., 1983). However, the application of negative pressure leads to significant blood contamination in approximately 80% of CSF samples (Fleming et al., 1983). Moreover, if not done carefully, it can even lead to the aspiration of a piece of soft brain tissue (Sakic, 2019). In the second study, CSF was collected from three substrains of hypermature mice (MRL/MpJ-Faslpr/J, MRL/MpJFaslpr/2 J, and MRL/MpJ) that had higher than average body mass at a young age and obtained of $\sim10\,\mu L$ of CSF from anesthetized mice and $\sim5\,\mu L$ of CSF from euthanized mice (Sakic, 2019). This discrepancy in the volume of CSF collected was proposed to be accounted for by the collapse of the cisternal space in euthanized mice (Sakic, 2019). In this study, several extractions of CSF from the same mouse were performed. The first CSF was obtained by capillary forces while for the next draws, the authors aspirate the CSF. We noticed, in agreement with their observations, that the first draw often gives the cleanest CSF, while secondary and tertiary draws, besides yielding smaller volumes due to the loss of intracranial pressure and heartbeat (Sakic, 2019), are often characterized by small air bubbles and carry a great risk of blood/brain tissue contamination. On the contrary, our simple procedure only contemplates *one single draw from each mouse* and it represents an efficient method to produce non-contaminated CSF samples. After many tests, in order to achieve the best combination of sampling robustness and efficiency, still devoid of blood contamination, we modified and optimized a procedure previously described (Liu and Duff, 2008). The Materials and Methods section fully described the final CSF sampling procedure we used. With this protocol, the CSF collection yields a clear, transparent fluid. When penetrating the *dura mater* with the capillary tube, lateral to the *arteria dorsalis spinalis,* it is important to avoid the blood vessels, in order to prevent blood contamination. Fig. 1, Panel A shows the glass microcapillary pipettes used for this study. Panel B indicates the exact point in mouse anatomy where puncture should be performed in order to optimize the whole procedure and avoid blood contaminations. The collected CSF is then expelled into a tube by connecting the pipette to a 1 mL syringe through a microcapillary holder (Fig. 1, Panel C).

Thanks to the sensitivity of the LC–MS/MS method, the amount of collected volume is knowingly sacrificed to minimize the risk of blood contamination. After allowing some time to familiarize with it, this procedure allows the operator to confidently sample 1–2 µL of perfectly clean mouse CSF from 90 to 95% of the animals.

2.2. LC–MS/MS method optimization

2.2.1. Chromatographic setup

After testing a plethora of stationary phases from different vendors, with only few of them showing retention for some of these compounds, we decided for an ion-pairing strategy to enhance NM retention. HFBA, a very well-known modifier (Chaimbault et al., 1999; Rao et al., 1999; Xie et al., 2013) was tested first. While most of the analytes elute in the void volume of the column, when using HFBA all of them are retained on column, although with non-optimal peak shape and separation. We then tried two other modifiers with longer carbon chains: nonafluoropentanoic acid (NFPA) and pentadecafluorooctanoic acid (PFOA). Both of them are volatile and suitable for MS, but have been much less
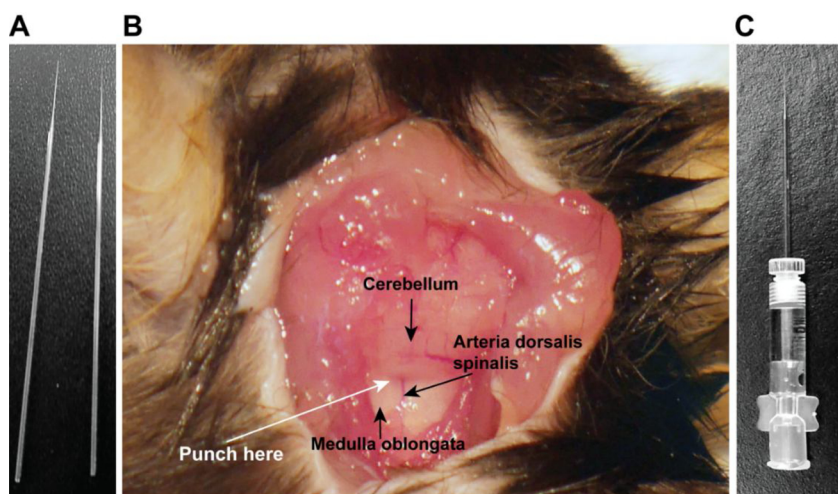
Fig. 1. (A) Glass micro-capillary pipettes with the pulled tip that were used to penetrate the tissue and collect the CSF. (B) Picture showing the cisterna magna after the skin and the muscles of the neck were removed. We used the glass needle (A) to punch the exposed dura mater above the cisterna magna slightly lateral to the midline, as shown. (C) Micro-capillary holder that connected to a 1 mL syringe was used to expel the CSF in an Eppendorf tube.
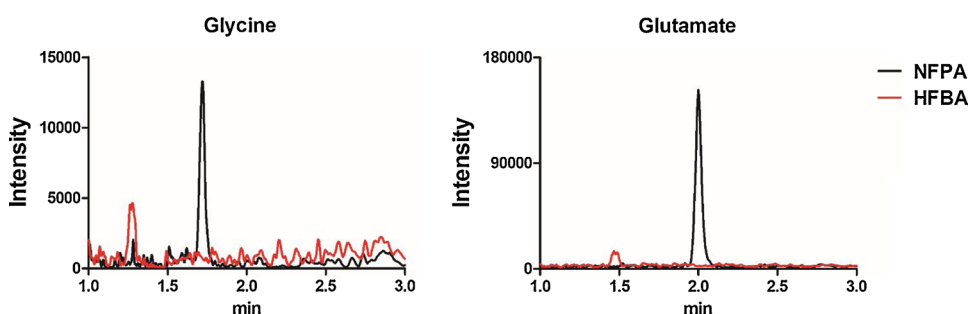

Fig. 2. Overlapped chromatograms of Glycine (left, 76 m/z → 30 m/z) and Glutamate (right, 148 m/z → 84 m/z) obtained with 0.1% HFBA (in red) and 5 mM NFPA (in black) as ion pairing reagents. The use of HFBA dramatically suppresses the ionization of these analytes. (For interpretation of the references to color in this figure legend, the reader is referred to the web version of this article.)

explored in RP-LC–MS/MS. The analysis with PFOA as ion pairing reagent needed longer equilibration time in order to obtain an adequate repeatability of the method, thus significantly increasing analysis time. This agent was therefore discarded. Both HFBA and NFPA provided good retention of the NM, however, the use of HFBA generated a stronger suppression effect for the AANM. Fig. 2 reports, as an example, the MRM chromatograms of glycine and glutamate obtained with HFBA and NFBA).

NFPA was then selected as the best overall performing ion-pairing agent. The NM separation was then optimized by comparing three concentrations of additive: 0.25, 2.5 and 5 mM. Lower concentrations of additives (besides facilitating the post-analysis cleaning of the instrument) produce lower signal suppression. However, the retention observed when using 0.25 mM of NFPA is not satisfactory, particularly for AANM, which coelute in the first minute of the run. Both 2.5 and 5 mM concentrations produce good separations for all NM, avoiding inter-analyte suppression. Therefore, an aqueous mobile phase with 0.1% HCOOH and 2.5 mM NFPA was selected as final condition for the analysis. The use of NFPA also allowed us to increase the sample throughput by shortening the gradient time from 1–50% in 8 min (Fig. 2) to 1–50% in 6 min (final LC–MS condition). The major drawback of the use of perfluorinated acids in RP-LC–MS/MS lies in the high suppression they cause in the negative ionization mode. HFBA (observed as 169 and 213 m/z ions in ESI-) is very well known in the chromatographic community for sticking to LC systems for long time after its removal and it is extremely difficult to wash it out at the end of the analytical session.

2.3. Method validation

Given the endogenous nature of these compounds, and the extremely low amount of CSF collected, we used artificial CSF (aCSF) as a surrogate matrix for the validation. Conventional aCSF, widely used and commercially available, only consists of K^+, Na^+, Ca^{++} and Mg^+

$^+$ chlorides and phosphates at different concentrations. It has indeed been demonstrated (Hooshfar et al., 2016) that such a composition, not accounting for proteins, shows non-negligible differences in recovery and matrix effects when compared to natural CSF. We then decided to use aCSF fortified with bovine serum albumin (BSA) and glucose, as already suggested in literature (Korecka et al., 2014) to better mimic the natural CSF composition and to validate our analytical method. Table 1 summarizes all the data related to the validation of the method, reporting the quantification range, the calibration linearity, as well as the calculated inter- and intra-day precision and accuracy values. Supplementary Fig. 1 reports the LC–MS/MS traces of the 10 µM calibrator. This validation step allowed us to test the robustness of our method on real mouse samples.

2.4. Application to real mouse samples

We sampled and analyzed the CSF of a total of 37 mice, weighing 14–35 g and ranging from 6 to 76 weeks of age. Supplementary Table 1 reports all the data collected on this sample set, including the glucose blood levels. As a representative example, Fig. 3 shows the MRM chromatograms obtained from the CSF of a 9 week old male mouse, where 11 out of the 12 analyzed NMs were detected with this method.

All the samples generated consistent NM data, with the exception of one (sample N°36), collected from a 6 weeks old female pup, that passed the visual inspection for blood contamination, but produced unusually high levels of NMs. For EP, ACh, and MHis, more than 50% of the values observed in our dataset were below our formally calculated LLOQ, but clearly visible in most of the samples, as demonstrated by Fig. 3. DA instead was not detected in this set of animals. Since, in our dataset, not all the features passed a D'Agostino–Pearson normality test (D'Agostino et al., 1990), we did not remove the sample from the set (Siebert and Siebert, 2018) but we highlighted it in red in Supplementary File 1. If we assume that this sample is non-reliable, then in a real-life experimental setup the practical observed failure rate of our

Table 1
Validation data for the LC–MS/MS method used for NM quantification: quantification range (upper and lower limits of quantification, linearity, accuracy and precision (both intra and interday).

|	Quan. range LLOQ–ULOQ	Linearity	Accuracy (% RE)						Precision (%RSD)					
			Intra-day			Inter-day			Intra-day			Inter-day		
	(µM)	(r^2)	Low	Mid	High	Low	Mid	High	Low	Mid	High	Low	Mid	High
Asp	$1-100$	0.999	3.05	6.00	3.28	5.09	5.02	3.19	3.50	7.02	3.37	5.92	5.43	3.25
Ser	$1-100$	0.994	3.24	4.71	3.80	5.69	5.26	3.44	3.95	5.28	3.67	6.75	5.66	3.07
Gly	$1-100$	0.997	4.25	4.50	4.33	5.30	4.49	3.06	4.80	6.07	5.44	6.19	5.35	4.15
Glu	$1-100$	0.996	11.28	4.18	2.34	11.54	3.72	1.97	9.73	5.28	2.95	7.43	4.49	2.50
GABA	$0.1-100$	0.999	11.17	4.83	3.88	12.69	3.31	2.64	14.68	4.63	2.65	14.81	4.25	3.31
NE	$0.1-100$	0.992	12.02	4.28	3.99	12.35	2.99	2.86	14.84	4.93	3.44	14.41	4.21	3.48
EP	$0.1-100$	0.997	9.32	6.26	4.29	13.07	4.09	3.13	8.50	7.77	3.80	14.15	4.06	3.69
DA	$0.1-100$	0.999	13.01	3.36	4.07	13.20	4.52	3.60	10.83	4.59	2.87	14.95	5.61	3.39
ACh	$0.1-100$	0.999	11.53	5.63	6.33	11.93	7.94	4.22	12.41	7.05	3.31	11.83	6.90	4.35
5 H T	$0.1-100$	0.991	8.92	5.13	3.54	10.66	3.71	3.66	0.45	6.00	4.30	5.67	4.51	4.48
His	$0.1-100$	0.99	12.12	4.24	5.43	12.36	5.00	4.45	13.61	4.22	5.20	14.60	6.03	4.20
MHis	$0.1-100$	0.977	8.79	12.51	5.82	7.98	9.18	3.61	7.61	4.33	4.41	9.11	8.07	3.85
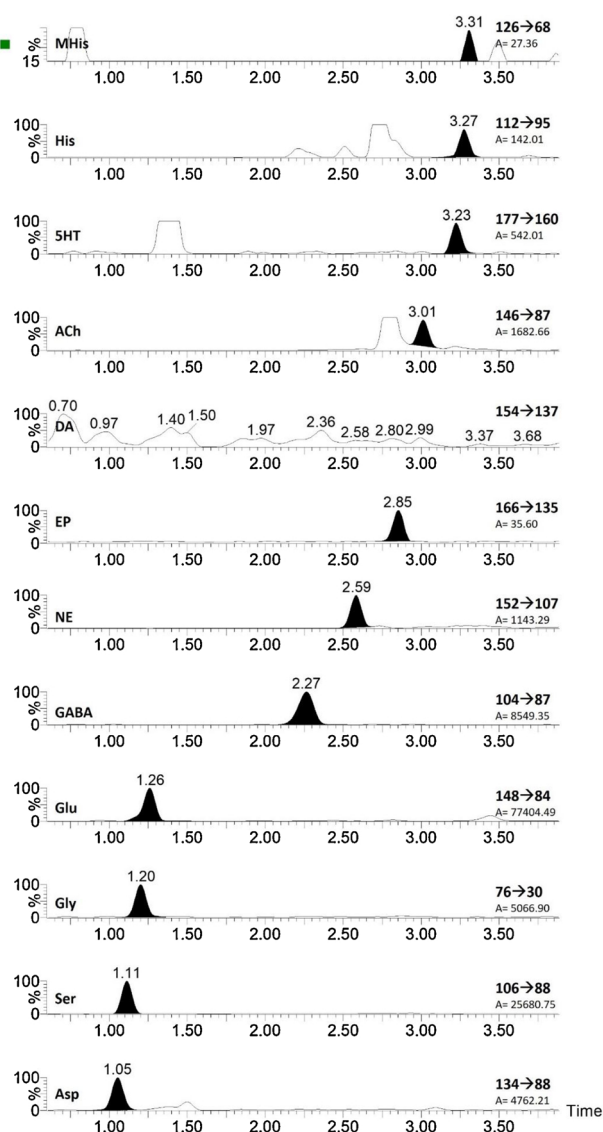
Fig. 3. LC–MS/MS chromatograms of NMs, with the indication of the MRM trace and the absolute area for each peak (A), obtained from a real sample of CSF obtained from a 9-week old male mouse (sample 24 in Supplementary Table 1).

method was 1/37, corresponding to less than 3% of samples passing the visual screening for blood contamination but producing unreliable results. We then investigated the results from the dataset, in order to derive some biologically relevant observation. Unfortunately, no literature data is available on this topic (NMs in mouse CSF), so our study represents a novelty in the field. We first performed a correlation analysis of our dataset, reported in Fig. 4, in order to have a general overview of the trends in our dataset. Data for EP, ACh, DA and MHis were removed.

CSF levels of GABA, Asp, Glu and Gly appear to be the most correlated with each other, and to a lesser extent, correlated with blood glucose levels. This is consistent since GABA is produced by Glu and it enters the TCA cycle through the GABA-shunt pathway (Cooper and Jeitner, 2016). In this process, through the action of 4-aminobutyrate aminotransferase (ABAT), glycine is produced from glyoxalate (Li et al., 2018). From TCA cycle, Asp is produced from oxaloacetate by the action of aspartate transaminase (AST) (Karmen et al., 1955). As glucose feeds the TCA cycle, from which Glu derives (through alpha-ketoglutarate), a correlation with blood glucose is also consistent. We also analyzed, mostly from a purely descriptive point of view, the trends with age of some of these metabolites and their ratio. Fig. 5 reports the trend with age of GABA (Panel A) and of the ratio between excitatory (Glu, Asp) and inhibitory (GABA, Gly) NMs (Panel B).

Supplementary Table 2 reports all the details for the correlation analysis we performed on the acquired data. Among all the analytes and combinations we tested, only glycine showed a weak negative correlation with mouse age ($p = 0.03$ Spearman $r = -0.35$). GABA shows a trend for decrease with age, although not significant. This is consistent with other studies in humans, showing a decline in GABA concentration in different brain areas in humans as a result of age (Gao et al., 2013; Porges et al., 2017). The exact relationship between GABA-mediated processes and behavioural performance across the lifespan has been the topic of several investigations (Porges et al., 2017; McQuail et al., 2015; Lasarge et al., 2009; Banuelos et al., 2014). Quite interestingly, we found that the ratio between excitatory and inhibitory NMs is stable with age. All the details about the correlation analyses of Fig. 4 and 5 are reported in Supplementary Table 2. The observed average values for the mouse population under analysis are reported in Table 3. No further correlations appear to be present in our dataset. We then compared the data obtained on our heterogeneous mice population (males and females specimens ranging from 6 weeks to 76 weeks of age) with other data on NMs CSF levels from rats and humans. This turned out to be a complicated task, because of the number of strains and models used for rats and the heterogeneity of the human population (age, sex, clinical condition) investigated in hundreds of neurological studies. All this results in a variety of different values reported in literature. For
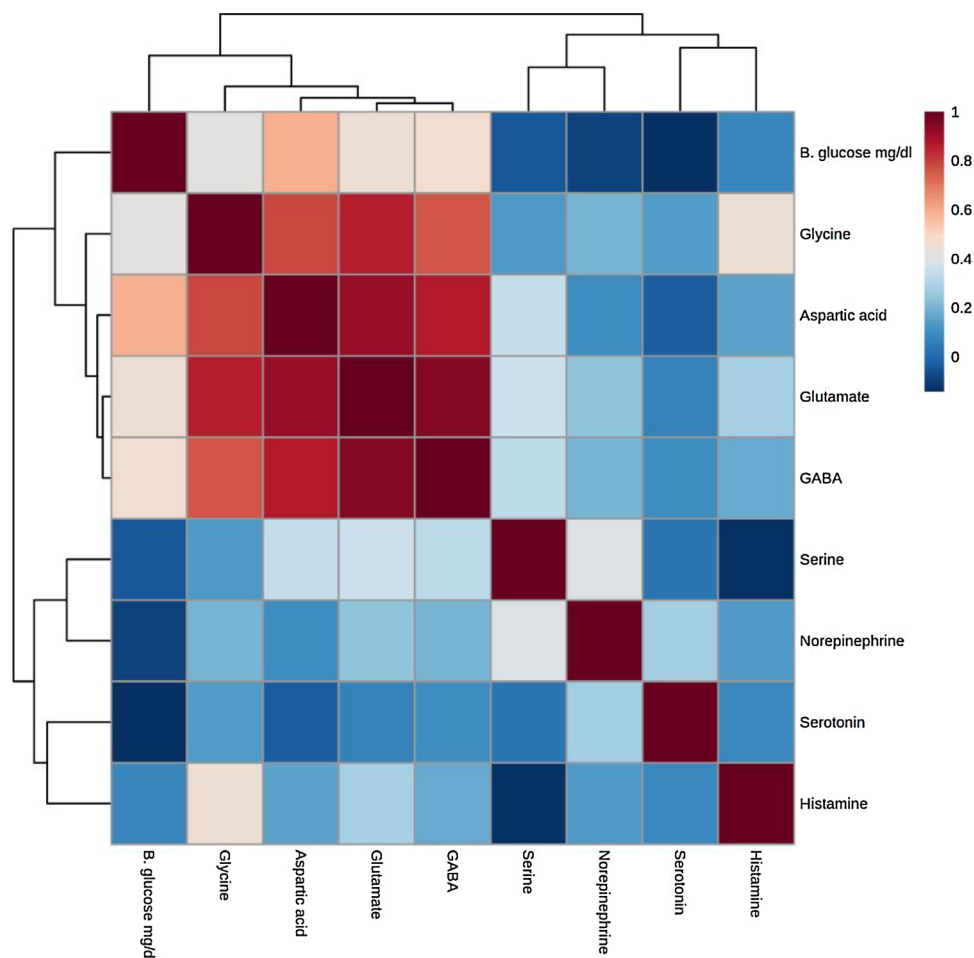
Fig. 4. Heatmap reporting Pearson's correlation analysis of the NM data obtained on the analyzed sample set, including blood glucose levels as feature. Data refer to 37 individual mice. NM with > 50% values lower than LLOQ were removed from the plot.

example, our extrapolated data on acetylcholine (average 30 nM) are remarkably similar to those reported by Togashi et al. (1994) in rats (slightly lower than 20 nM). Conversely, our GABA and Glu levels (4.0 and 31 μM on average) appear to be quite distant from those published for rats sacrificed (Martínez-Méndez et al., 2016) 3 days after birth (around 50 and 250 μM respectively). Other papers report very different values, closer to ours, like 4.8 μM (Stover and Unterberg, 2000) for Glu. As far as human CSF is concerned, data available in literature range from 0.09 μM (Perry et al., 1982) to 0.3 μM (Sourkes, 2010) for

GABA and from 6 to 17 μM for Glu (Madeira et al., 2018), values similar to ours. More complicated is to find reference values for other NMs, as very few papers like ours report data on several NMs simultaneously. In conclusion, in the present paper, we introduce a novel, sensitive, robust and straightforward method for the simultaneous analysis of a panel of neuroactive molecules (12) from mouse CSF. Unlike most methods available in literature, that normally focus on a restricted set of analytes, our method is able to investigate all the most important NMs simultaneously: inhibitory and excitatory, both aminoacids and
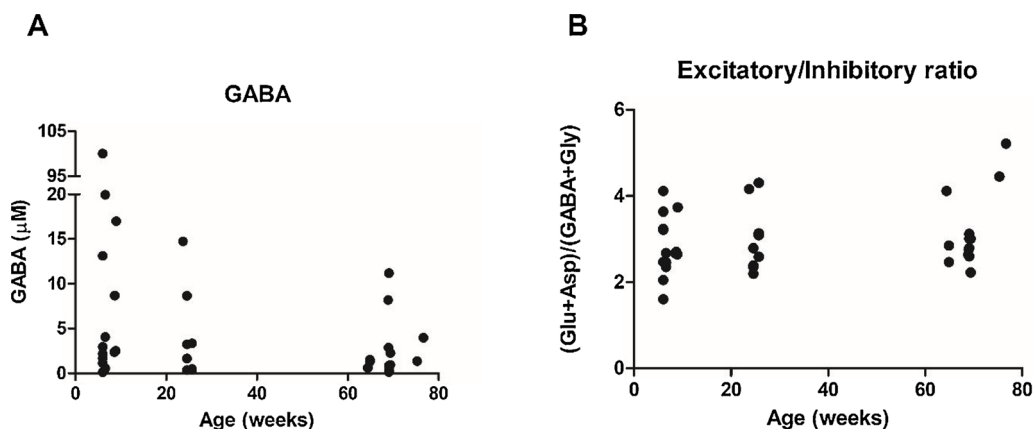

Fig. 5. Trends with age of CSF GABA levels (A) and CSF Excitatory/inhibitory NMs ratio (B), Glu + Asp/GABA + Gly. Data refer to 37 individual mice. No significant trends were observed in the data (Spearman p-value > 0.05).

Table 2

Brute formula, molecular weight, LogP values and LC–MS/MS parameters for the analytes under investigation. The MRM traces used for quantification are underlined.

Type of NM	Analyte	Abb.	Molecular formula	MW	LogP*	Rt	MRM Transitions	CV (V)	CE (eV)
AANM	Aspartate	Asp	$C_4H_7NO_4$	133.1	−3.89	1.06	<u>134 > 88</u>	10	10
							134 > 74	10	10
	Serine	Ser	$C_3H_7NO_3$	105.1	−3.07	1.13	<u>106 > 88</u>	15	10
							106 > 60	15	10
	Glycine	Gly	$C_2H_5NO_2$	75.1	−3.21	1.21	<u>76 > 30</u>	15	5
							76 > 48	15	5
	Glutamate	Glu	$C_5H_9NO_4$	147.1	−3.69	1.28	<u>148 > 84</u>	15	15
							148 > 130	15	10
	Glutamate-2,3,3,4,4-d5	Glu-d5	$C_5H_4D_5NO_4$	152.1	–	1.28	153 > 99	20	20
	γ-Amminobutiric acid	GABA	$C_4H_9NO_2$	103.1	−3.17	2.34	104 > 69	20	15
							<u>104 > 87</u>	20	10
	γ-Amminobutiric acid-2,2,3,3,4,4-d6	GABA-d6	$C_4H_3D_6NO_2$	109.1	–	2.34	110 > 93	20	10
MANM	Norepinephrine	NE	$C_8H_{11}NO_3$	169.2	−1.24	2.61	<u>152 > 107</u>	25	15
							152 > 135	25	10
	Epinephrine	EP	$C_9H_{13}NO_3$	183.2	−1.37	2.87	166 > 107	30	20
							<u>166 > 135</u>	30	15
	Dopamine	DA	$C_8H_{11}NO_2$	153.2	−0.98	3.03	154 > 91	15	20
							<u>154 > 137</u>	15	10
ACh	Acetylcholine	ACh	$C_7H_{16}NO_2$	146.2	0.2	3.03	87 > 43	40	35
							<u>146 > 87</u>	20	15
MANM	Serotonin	5 H T	$C_{10}H_{12}NO_2$	176.2	0.21	3.24	177 > 115	15	25
							<u>177 > 160</u>	15	10
	Histamine	His	$C_5H_9N_3$	111.1	−0.7	3.29	112 > 68	20	20
							<u>112 > 95</u>	20	10
	Histamine-α,α,β,β-d4	His-d4	$C_5H_5D_4N_3$	115.1	–	3.33	116 > 99	20	15
	Methyl Histamine	MHis	$C_5H_{11}N_3$	125.2	−0.6	3.29	<u>126 > 68</u>	20	15
							126 > 109	20	5

* Log P values obtained from Pubchem database. Underlined transitions were used for quantification.

Table 3

Overall average values for the mouse population under investigation (37 animals). The Table reports the data for those analytes we were able to quantify in the mouse population under investigation.

Units	Variable	Average values	Standard deviation
Weeks	Age	33.2	27.5
Grams	Weight	25.4	5.8
mg/dL	Glycemia	168	28
Micromolar	Aspartic acid	10.30	16.98
	Serine	40.11	13.77
	Glycine	11.95	17.02
	Glutamate	36.33	41.39
	GABA	6.64	16.35
	Norepinephrine	0.279	0.10
	Epinephrine	< LLOQ	N/A
	AcetylCholine	< LLOQ	N/A
	Dopamine	< LLOQ	N/A
	Serotonin	0.388	0.320
	Histamine	0.220	0.110
	Metylhistamine	0.163	0.060

monoamines. We extensively tested out method on-the-field, by analyzing the CSF of 37 individual mouse specimens of different sex and age. To the best of our knowledge, this is the first time that a paper reports on NM quantification from *mouse* CSF. Still, despite the absence of relevant literature on NM concentration in this biofluid, our data are consistent with current knowledge about mammalian brain metabolism and our values are generally in line with those observed in rats and humans. Thanks to the downstream sensitivity of the LC–MS/MS detection, our animal sampling method deliberately sacrifices the amount of CSF collected from a single specimen to lower the risk of blood contaminations and ensure its cleanliness and purity. Furthermore, after CSF collection, the absence of any sample preparation (dilute & analyse) makes the overall process extremely straightforward and easy. Despite the high sensitivity of the developed method, this was not enough for the reliable quantification of some of the metabolites in lowest concentrations in this biological fluid as dopamine, epinephrine or

acetylcholine in *naïve* animals. However, it opens a promising door for future analysis of samples taken from mice with altered levels of these neuroactive molecules, until now unexplored. If routinely implemented, our method will allow the quantitative measurement of NM variation across a wide range of neurological conditions. Given the novelty of our work, we are confident that our method will pave new ways for the investigation of brain physiology and neurology, thanks to the number of mouse model that are currently used in this field.

3. Materials and methods

3.1. Chemicals and materials

The twelve metabolites (5-Hydroxytryptamine Hydrochloride, Acetylcholine chloride, ʟ-aspartic acid, 3-Hydroxytyramine hydrochloride, (±)Epinephrine hydrochloride, γ-Aminobutyric acid, ᴅ-Glutamic acid, Glycine, Histamine dihydrochloride, Methyl-Histamine, ᴅʟ-Norepinephrine hydrochloride, ᴅ-Serine), perfluorocarboxylic acids (pentadecafluorooctanoic acid, nonafluoropentanoic acid and 2,2,3,3,4,4,4-heptafluorobutanoic acid) and internal standards (IS) with isotope labeling (4-Aminobutyric acid-2,2,3,3,4,4-d6, ʟ-Glutamic acid-2,3,3,4,4-d5 and Histamine-α,α,ß,ß-d4) were purchased from Sigma-Aldrich. Formic acid for LC–MS from Merck (Darmstadt, Germany) was used. LC–MS grade acetonitrile was purchased from Honeywell (Charlotte, NC, USA). Water was purified using a Milli-Q water purification system from Millipore (Bedford, MA, USA). The glass capillary tube used for CSF sampling was purchased from The Sutter Instrument Inc (Borosilicate glass, B100-75-10). Micro-capillary pipettes are prepared by applying heat and pull using a Narishige PC-10 vertical micropipette puller with the following settings: One step pull; Heater #2 set to 58; 100 g pull weight. The fine tip of the micropipette is carefully snapped off using fine #55 forceps. The microcapillary holder was purchased from World Precision Instruments (MPH6S12).

3.2. Preparation of standard solutions

Individual stock solutions (10 mM) of each NM were prepared in water. A mixed working solution at 100 µM was prepared by diluting the stock solutions with artificial CSF (aCSF; 150 mM Na^+, 3 mM K^+, 1.4 mM Ca^{++}, 0.8 mM Mg^{++}, 1 mM $H_2PO_4^-$, 155 mM Cl^-, 10 mM glucose, 0.5 mg mL^{-1} bovine serum albumin). Calibration solutions where prepared by further dilution with aCSF. Stock and working solutions were kept at $-20\,°C$ when not in use, while calibration solutions where freshly prepared the day of analysis.

3.3. Animals

All experiments and procedures involving mice were approved by the IIT Animal Use Committee and the Italian Ministry of Health (Permit No. 176AA.N.U3R, rif IIT No 129, approved on Jan 18th, 2018). All animal experiments were conducted in accordance with the Guide for the Care and Use of Laboratory Animals of the European Community (Directive 2010/63/EU) and Italian guidelines (D.Lgs 26/2014). Mice from C57/Bl6 strain were obtained from (Charles River) and housed with ad libitum access to food and water and kept on a 12 h (8 A.M. to 8 P.M.) light-dark cycle, in a room maintained at 21 °C at the animal facility of the Istituto Italiano di Tecnologia. The day of birth was considered as postnatal day 0 (P0). Mice were weighed on a desktop scale and injected intraperitoneally with an adequate volume ($\sim$ 0.2 mL) of fresh ketamine (100 mg kg^{-1}) /xylazine (10 mg kg^{-1}) cocktail. All CSF samples were collected at 1 P M ($+/-$ 1 h).

3.4. Surgical procedure and CSF sampling

The CSF was collected from *cisterna magna* of euthanized C57 mice (6–76 weeks of age, both male and female). The most challenging part of the workflow consists in the surgical procedure that allows access to the *cisterna magna* of the mice. The protocol for sampling of CSF from mice is developed by modification of the methodological procedure from Liu and Duff (2008). After sacrifice, the animal is placed prone on a stereotaxic instrument with the head secured with the head adaptors forming a nearly 45° angle with the body. This allows the *dura mater* of *cisterna magna* to be sufficiently exposed. The surgical site is swabbed with 70% ethanol and a sagittal incision of the skin is made inferior to the occiput. Under the dissection microscope, the subcutaneous tissue and muscles (m. *biventer cervicis* and m. *rectus capitis dorsalis major*) are separated by blunt dissection with forceps exposing the meninges above the *cisterna magna* (Fig. 1). After careful dissection and muscle removal, to avoid bleeding during the sampling, the atlanto-occipital membrane above the *cisterna magna* will appear as a reverse triangle through which are visible the *medulla oblongata*, a major blood vessel (*arteria dorsalis spinalis*) and the CSF space (Fig. 1). Cotton swabs were used to remove interstitial fluid in the incision area before the CSF draw. Then, a glass micro-capillary pipette with a pulled tip was used to create an ultrafine point for improved tissue penetration (Fig. 1, Panel A). An elongated, sharp tip easily punctures the *atlanto-occipital membrane/dura*, allows capillary forces to assist in the first CSF draw as well as the continuously monitoring the CSF flow visually. The capillary tube is carefully inserted into the *cisterna magna* through the *dura mater,* lateral to the *arteria dorsalis spinalis* (Fig. 1, Panel B). Following a noticeable change in resistance to the capillary tube insertion, the CSF flows into the capillary tube due to capillary forces and inner pressure. With this procedure, the CSF collection yields a clear, transparent fluid. When penetrating the *dura mater* with the capillary tube, it is important to avoid the blood vessels, in order to prevent blood contamination. Once the CSF is collected, the capillary tube is carefully removed and connected to a 1 mL syringe through a microcapillary holder (see Fig. 1, Panel C) that has 1.2 mm of internal diameter. Then, the CSF is gently expelled into a pre-marked eppendorf tube that has been chilled on ice. Finally, the sample is centrifuged at 10,000x*g* at 4 °C for 1 min to remove any contaminating cells. Blood contamination is checked by placing white paper below the glass pipette and vial after centrifugation. Previous studies have demonstrated that visual inspection allows to identify as little as 0.05% blood contamination (You et al., 2005). Visual inspection revealed that > 95% of CSF samples collected with this protocol are perfectly clean. Only clear, uncontaminated samples were used in our study. The collected sample are then snap frozen with liquid nitrogen and stored at $-80\,°C$ until the time of analysis. The entire procedure takes approximately $10-15$ min per sample (including anaesthesia, CSF collection, centrifugation and quality inspection) and usually results in the collection of $1-2\,µL$ of extremely clean and blood free mouse CSF.

3.5. Blood glucose measurement

Blood was obtained from a tail cut and glucose levels were assessed using an OneTouch Ultra 2 (LifeScan, Johnson & Johnson) glucometer.

3.6. Sample handling and preparation

As the amount of CSF obtained with this procedure is very low, no analyte extraction steps were taken into account. Instead, samples are diluted in order to reach a volume suitable to be handled by the LC–MS/MS system. For every sample collected, 1 microliter of CSF was precisely and accurately collected with a 2 µl precision pipette and transferred to a 0.5 mL Eppendorf tube and stored until analysis. For method validation, 1 microliter of aCSF was collected. The day of analysis, after thawing, 9 µL of an aqueous solution of 0.1% HCOOH spiked with the IS at a concentration of 200 nM were thus simply added to the CSF sample (1 µL). Diluted samples were then vortex mixed and then centrifuged at 4 °C and 20,000x*g* for 10 min. The total absence of intermediate processing steps makes this part of the procedure extremely simple and fast.

3.7. LC–MS/MS chromatographic method

LC–MS/MS separation was performed using a Waters Acquity UPLC system coupled to a Xevo TQ-MS triple quadrupole mass spectrometer, equipped with an electrospray ionization (ESI) source working in positive mode and controlled by the MassLynx software. The separation was achieved on a ACE Excel 2 C18-AR (150 × 2.1 mm) column (Advanced Chromatography Technologies Ltd, Aberdeen, Scotland) with the following eluent system: A = 0.1% HCOOH, 2.5 mM NFPA in water and B = ACN. A linear gradient (1–50% B in 6 min) was used, with a flow rate of 0.5 mL min^{-1}. The injection volume was set to 4 microliters.

3.8. MS parameters

Mass spectrometer source temperature was set at 150 °C. Nitrogen was used as desolvation (800 L h^{-1}, 450 °C) and collision gas. To carefully tune the source parameters for each of the 12 analytes, 10 µM solutions of each NM in 0.1% HCOOH were infused into the MS. Data was acquired in multiple reaction monitoring mode (MRM) mode, using two transitions (one for quantification, the other for confirmation of the identification) for each compound. The cone voltages (CV) and collision energies (CE) for each transition were optimized in order to achieve the maximum response. Table 2 reports the observed retention times and MS source parameters and MRM transitions used for the detection of the analytes, along with their molecular weight and LogP values.

3.9. Method validation

The method was validated following the FDA guidelines (Tsikas, 2018; Gonzalez et al., 2014) in terms of linearity, sensitivity, accuracy, precision, carryover and matrix effect. Artificial CSF was used as

surrogate matrix. Calibration solutions were prepared by spiking the aCSF with the working solution. Three calibration ranges were prepared 0.1–1, 1–10 and 10–100 μM, each one consisting of a blank sample (blank aCSF), a zero sample (blank aCSF spiked with the IS), and 8 non-zero calibration standards. Calibration curves were built by plotting the peak area of the analyte divided by the peak area of the corresponding IS against the nominal concentration. The IS corresponding to each NM was selected based on retention time and matrix effect criteria. Therefore, Glu-d5 is used as IS for Asp, Ser, Gly and Glu; GABA-d6 is used for GABA, NE, EP, DA, ACh, and 5 H T; His-d4 is used as IS for His and MHis. The curve was considered valid if the deviation from the nominal concentration of at least 5 out of 8 calibration standards (except blank and zero samples) was lower than 15% (20% for the LLOQ). The lower point of the curve complying with these requirements was considered the lower limit of quantitation (LLOQ). The selectivity of the method was validated by comparing the response of six aliquots of aCSF with the analytes at LLOQ. According to the FDA, the signal obtained in the blank matrix should be lower than 20% the signal of the analyte at the LLOQ and lower than 5% the signal of the IS. Five spiked samples at three levels of concentration as quality control (QC) samples (Low, Mid and High QC) were analyzed the same day and in three different days in order to calculate intra- and inter-day accuracy of the calculated concentrations. Accuracy was calculated as relative error (%RE) of the concentration obtained from interpolation of the corrected area in the calibration curve against its nominal concentration. Accuracy was considered acceptable if%RE < 15%. Five replicates of the same Low, Mid and High QC were used to test intra- and inter-day precision, by evaluation of the relative standard deviation (%RSD) of their calculated concentrations. The acceptance criterion was%RSD < 15%. Carryover was considered acceptable if the response of a blank sample injected immediately after the highest calibration point was below 20% the signal at the LLOQ and below 5% the IS signal. The qualitative evaluation of the matrix effect was performed by post column infusion experiments, infusing post column 10 μM solutions of each compound individually while simultaneously injecting blank samples.

3.10. Data analysis

Peak integration and NM quantification were performed using Targetlynx software (Waters). Smoothed peaks (Mean, iterations: 3, smooth width: 2) were automatically integrated by ApexTrack integration, and manually inspected and corrected if necessary. Correlation analysis (Fig. 4) was performed using MetaboAnalyst software (Xia and Wishart, 2016) in the dimension of the features (the 12 NMs) and using Pearson distance. Data were not normalized or transformed.

Data availability

All the RAW and result files related to the present work are freely available at any time upon request to the corresponding author.

Funding

CRediT authorship contribution statement

María Encarnación Blanco: Investigation, Methodology. **Olga Barca Mayo:** Investigation, Methodology. **Tiziano Bandiera:** Data curation, Writing - review & editing. **Davide De Pietri Tonelli:** Data curation, Writing - review & editing. **Andrea Armirotti:** Supervision, Visualization, Writing - original draft.

Declaration of Competing Interest

The authors declare no conflicts of interest of any kind

Appendix A. Supplementary data

Supplementary material related to this article can be found, in the online version, at doi:https://doi.org/10.1016/j.jneumeth.2020.108760.

References

Banuelos, C., et al., 2014. Prefrontal cortical GABAergic dysfunction contributes to age-related working memory impairment. J. Neurosci. 34, 3457–3466. https://doi.org/10.1523/JNEUROSCI.5192-13.2014.

Bernabo, N., Barboni, B., Maccarrone, M., 2013. Systems biology analysis of the endocannabinoid system reveals a scale-free network with distinct roles for anandamide and 2-arachidonoylglycerol. OMICS 17, 646–654. https://doi.org/10.1089/omi.2013.0071.

Bovingdon, M.E., Webster, R.A., 1994. Derivatization reactions for neurotransmitters and their automation. J. Chromatogr. B, Biomed. Appl. 659, 157–183.

Bowery, N.G., Smart, T.G., 2006. GABA and glycine as neurotransmitters: a brief history. Br. J. Pharmacol. 147 (Suppl 1), S109–119. https://doi.org/10.1038/sj.bjp.0706443.

Bruno, G., et al., 1995. Acetyl-ʟ-carnitine in Alzheimer disease: a short-term study on CSF neurotransmitters and neuropeptides. Alzheimer Dis. Assoc. Disord. 9, 128–131.

Cai, H.L., Zhu, R.H., Li, H.D., 2010. Determination of dansylated monoamine and amino acid neurotransmitters and their metabolites in human plasma by liquid chromatography-electrospray ionization tandem mass spectrometry. Anal. Biochem. 396, 103–111. https://doi.org/10.1016/j.ab.2009.09.015.

Carr, R., Frings, S., 2019. Neuropeptides in sensory signal processing. Cell Tissue Res. 375, 217–225. https://doi.org/10.1007/s00441-018-2946-3.

Chaimbault, P., Petritis, K., Elfakir, C., Dreux, M., 1999. Determination of 20 underivatized proteinic amino acids by ion-pairing chromatography and pneumatically assisted electrospray mass spectrometry. J. Chromatogr. A 855, 191–202.

Cooper, A.J., Jeitner, T.M., 2016. Central role of glutamate metabolism in the maintenance of nitrogen homeostasis in normal and hyperammonemic brain. Biomolecules 6. https://doi.org/10.3390/biom6020016.

Cox, J.M., et al., 2015. A validated LC-MS/MS method for neurotransmitter metabolite analysis in human cerebrospinal fluid using benzoyl chloride derivatization. Bioanalysis 7, 2461–2475. https://doi.org/10.4155/bio.15.170.

D'Agostino, R.B., Belanger, A., D'agostino Jr, R.B., 1990. A suggestion for using powerful and informative tests of normality. Am. Stat. 44, 316–321.

Dang, P.T., Bui, Q., D'Souza, C.S., Orian, J.M., 2015. Modelling MS: chronic-relapsing EAE in the NOD/Lt mouse strain. Curr. Top. Behav. Neurosci. 26, 143–177. https://doi.org/10.1007/7854_2015_378.

de Jong, P.J., Lakke, J.P., Teelken, A.W., 1984. CSF GABA levels in Parkinson's disease. Adv. Neurol. 40, 427–430.

Doummar, D., et al., 2018. Monoamine neurotransmitters and movement disorders in children and adults. Rev. Neurol. (Paris) 174, 581–588. https://doi.org/10.1016/j.neurol.2018.07.002.

Fleming, J.O., Ting, J.Y., Stohlman, S.A., Weiner, L.P., 1983. Improvements in obtaining and characterizing mouse cerebrospinal fluid. Application to mouse hepatitis virus-induced encephalomyelitis. J. Neuroimmunol. 4, 129–140.

Gao, F., et al., 2013. Edited magnetic resonance spectroscopy detects an age-related decline in brain GABA levels. NeuroImage 78, 75–82. https://doi.org/10.1016/j.neuroimage.2013.04.012.

Gibson, C.J., Logue, M., Growdon, J.H., 1985. CSF monoamine metabolite levels in Alzheimer's and Parkinson's disease. Arch. Neurol. 42, 489–492.

Gonzalez, R.R., Fernandez, R.F., Vidal, J.L.M., Frenich, A.G., Perez, M.L.G., 2011. Development and validation of an ultra-high performance liquid chromatography-tandem mass-spectrometry (UHPLC-MS/MS) method for the simultaneous determination of neurotransmitters in rat brain samples. J. Neurosci. Methods 198, 187–194. https://doi.org/10.1016/j.jneumeth.2011.03.023.

Gonzalez, O., et al., 2014. Bioanalytical chromatographic method validation according to current regulations, with a special focus on the non-well defined parameters limit of quantification, robustness and matrix effect. J. Chromatogr. A 1353, 10–27. https://doi.org/10.1016/j.chroma.2014.03.077.

Han, X., et al., 2018. Quantitative profiling of neurotransmitter abnormalities in brain, cerebrospinal fluid, and serum of experimental diabetic encephalopathy male rat. J. Neurosci. Res. 96, 138–150. https://doi.org/10.1002/jnr.24098.

Hooshfar, S., Basiri, B., Bartlett, M.G., 2016. Development of a surrogate matrix for cerebral spinal fluid for liquid chromatography/mass spectrometry based analytical methods. Rapid Commun. Mass Spectrom. 30, 854–858. https://doi.org/10.1002/rcm.7509.

Hyland, K., 2008. Clinical utility of monoamine neurotransmitter metabolite analysis in cerebrospinal fluid. Clin. Chem. 54, 633–641. https://doi.org/10.1373/clinchem.2007.099986.

Inoue, K., et al., 2016. Stable isotope dilution HILIC-MS/MS method for accurate quantification of glutamic acid, glutamine, pyroglutamic acid, GABA and theanine in

mouse brain tissues. Biomed. Chromatogr. 30, 55–61. https://doi.org/10.1002/bmc.3502.

Jiang, J., James, C.A., Wong, P., 2016. Bioanalytical method development and validation for the determination of glycine in human cerebrospinal fluid by ion-pair reversed-phase liquid chromatography-tandem mass spectrometry. J. Pharm. Biomed. Anal. 128, 132–140. https://doi.org/10.1016/j.jpba.2016.05.019.

Karmen, A., Wroblewski, F., Ladue, J.S., 1955. Transaminase activity in human blood. J. Clin. Invest. 34, 126–131. https://doi.org/10.1172/JCI103055.

Karrenbauer, B.D., et al., 2011. Time-dependent in-vivo effects of interleukin-2 on neurotransmitters in various cortices: relationships with depressive-related and anxiety-like behaviour. J. Neuroimmunol. 237, 23–32. https://doi.org/10.1016/j.jneuroim.2011.05.011.

Korecka, M., et al., 2014. Qualification of a surrogate matrix-based absolute quantification method for amyloid-beta(4)(2) in human cerebrospinal fluid using 2D UPLC-tandem mass spectrometry. J. Alzheimers Dis. 41, 441–451. https://doi.org/10.3233/JAD-132489.

Kuriyama, K., Ohkuma, S., 1995. Role of nitric oxide in central synaptic transmission: effects on neurotransmitter release. Jpn. J. Pharmacol. 69, 1–8.

Lasarge, C.L., Banuelos, C., Mayse, J.D., Bizon, J.L., 2009. Blockade of GABA(B) receptors completely reverses age-related learning impairment. Neuroscience 164, 941–947. https://doi.org/10.1016/j.neuroscience.2009.08.055.

Li, R., et al., 2018. Multiplexed CRISPR/Cas9-mediated metabolic engineering of gamma-aminobutyric acid levels in Solanum lycopersicum. Plant Biotechnol. J. 16, 415–427. https://doi.org/10.1111/pbi.12781.

Liu, L., Duff, K., 2008. A technique for serial collection of cerebrospinal fluid from the cisterna magna in mouse. J. Vis. Exp. https://doi.org/10.3791/960.

Lodish, H.B., Zipursky, A., 2000. In: Freeman, W.H. (Ed.), Molecular Cell Biology.

Madeira, C., et al., 2018. Elevated glutamate and glutamine levels in the cerebrospinal fluid of patients with probable Alzheimer's disease and depression. Front. Psychiatry 9, 561. https://doi.org/10.3389/fpsyt.2018.00561.

Marsavelski, A., Vianello, R., 2017. What a difference a methyl group makes: the selectivity of monoamine oxidase B towards histamine and N-methylhistamine. Chemistry 23, 2915–2925. https://doi.org/10.1002/chem.201605430.

Martínez-Méndez, R., P.-C. P, Gómez-Chavarín, M., Gutiérrez-Ospina, G., 2016. Glutamate, GABA and serotonin concentrations in the cerebrospinal fluid and primary somatosensory cortex of birth-enucleated rats: searching for S1 intrinsic and extrinsic epigenetic regulatory signals modulating neonatal cross-modal plasticity. PeerJ PrePrints 4, e1782v1.

McQuail, J.A., Frazier, C.J., Bizon, J.L., 2015. Molecular aspects of age-related cognitive decline: the role of GABA signaling. Trends Mol. Med. 21, 450–460. https://doi.org/10.1016/j.molmed.2015.05.002.

Noriega-Ortega, B.R., et al., 2011. GABA and dopamine release from different brain regions in mice with chronic exposure to organophosphate methamidophos. J. Toxicol. Pathol. 24, 163–168. https://doi.org/10.1293/tox.24.163.

Pardridge, W.M., 2016. CSF, blood-brain barrier, and brain drug delivery. Expert Opin. Drug Deliv. 13, 963–975. https://doi.org/10.1517/17425247.2016.1171315.

Perry, T.L., Hansen, S., Wall, R.A., Gauthier, S.G., 1982. Human CSF GABA concentrations: revised downward for controls, but not decreased in Huntington's chorea. J. Neurochem. 38, 766–773.

Pirola, C.J., 1988. [Neurotransmitters as intracellular mediators during embryo development]. Medicina (B Aires) 48, 326–327.

Porges, E.C., et al., 2017. Frontal gamma-aminobutyric acid concentrations are associated with cognitive performance in older adults. Biol. Psychiatry Cogn. Neurosci. Neuroimaging 2, 38–44. https://doi.org/10.1016/j.bpsc.2016.06.004.

Ramakrishnan, R., Namasivayam, A., 1995. Norepinephrine and epinephrine levels in the brain of alloxan diabetic rats. Neurosci. Lett. 186, 200–202.

Rao, R.M., Rao, Y.M., Shah, A.H., 1999. A reverse phase ion-pairing HPLC method for the stability monitoring of sulphacetamide ophthalmic preparations. J. Pharm. Biomed.

Anal. 20, 717–722.

Rodan, L.H., Gibson, K.M., Pearl, P.L., 2015. Clinical use of CSF neurotransmitters. Pediatr. Neurol. 53, 277–286. https://doi.org/10.1016/j.pediatrneurol.2015.04.016.

Sakic, B., 2019. Cerebrospinal fluid collection in laboratory mice: literature review and modified cisternal puncture method. J. Neurosci. Methods 311, 402–407. https://doi.org/10.1016/j.jneumeth.2018.09.025.

Siebert, C.F., Siebert, D.C., 2018. Data analysis with small samples and non-normal data: nonparametrics and other strategies. Choice Current Rev. Acad. Libraries 56, 89-89.

Simon, M.J., Iliff, J.J., 2016. Regulation of cerebrospinal fluid (CSF) flow in neurodegenerative, neurovascular and neuroinflammatory disease. Biochim. Biophys. Acta 1862, 442–451. https://doi.org/10.1016/j.bbadis.2015.10.014.

Sourkes, T.L., 2010. Chapter 54: the discovery of neurotransmitters, and applications to neurology. Handb. Clin. Neurol. 95, 869–883. https://doi.org/10.1016/S0072-9752(08)02154-4.

Stover, J.F., Unterberg, A.W., 2000. Increased cerebrospinal fluid glutamate and taurine concentrations are associated with traumatic brain edema formation in rats. Brain Res. 875, 51–55.

Sustkova-Fiserova, M., Vavrova, J., Krsiak, M., 2009. Brain levels of GABA, glutamate and aspartate in sociable, aggressive and timid mice: an in vivo microdialysis study. Neuro Endocrinol. Lett. 30, 79–84.

Temudo, T., et al., 2009. Evaluation of CSF neurotransmitters and folate in 25 patients with Rett disorder and effects of treatment. Brain Dev. 31, 46–51. https://doi.org/10.1016/j.braindev.2008.05.003.

Thiele, S.L., Warre, R., Nash, J.E., 2012. Development of a unilaterally-lesioned 6-OHDA mouse model of Parkinson's disease. J. Vis. Exp. https://doi.org/10.3791/3234.

Togashi, H., et al., 1994. Acetylcholine measurement of cerebrospinal fluid by in vivo microdialysis in freely moving rats. Jpn. J. Pharmacol. 66, 67–74.

Tsikas, D., 2018. Bioanalytical method validation of endogenous substances according to guidelines by the FDA and other organizations: basic need to specify concentration ranges. J. Chromatogr. B Analyt. Technol. Biomed. Life Sci. 1093–1094, 80–81. https://doi.org/10.1016/j.jchromb.2018.07.005.

Voehringer, P., Fuertig, R., Ferger, B., 2013. A novel liquid chromatography/tandem mass spectrometry method for the quantification of glycine as biomarker in brain microdialysis and cerebrospinal fluid samples within 5min. J. Chromatogr. B Anal. Technol. Biomed. Life Sci. 939, 92–97. https://doi.org/10.1016/j.jchromb.2013.09.011.

Wu, X., et al., 2018. A HILIC-UHPLC-MS/MS untargeted urinary metabonomics combined with quantitative analysis of five polar biomarkers on osteoporosis rats after oral administration of Gushudan. J. Chromatogr. B Anal. Technol. Biomed. Life Sci. 1072, 40–49. https://doi.org/10.1016/j.jchromb.2017.10.005.

Xia, J., Wishart, D.S., 2016. Using MetaboAnalyst 3.0 for comprehensive metabolomics data analysis. Curr. Protoc. Bioinform. 55https://doi.org/10.1002/cpbi.11. 14 10 11-14 10 91.

Xie, W., Qin, X., Teraoka, I., Gross, R.A., 2013. Comparison of retention behavior of oligolysine and oligoarginine in ion-pairing chromatography using heptafluorobutyric acid. Anal. Bioanal. Chem. 405, 9739–9746. https://doi.org/10.1007/s00216-013-7397-9.

You, J.S., et al., 2005. The impact of blood contamination on the proteome of cerebrospinal fluid. Proteomics 5, 290–296. https://doi.org/10.1002/pmic.200490084.

Zhang, M.L., Fang, C.W., Smagin, G., 2014. Derivatization for the simultaneous LC/MS quantification of multiple neurotransmitters in extracellular fluid from rat brain microdialysis. J. Pharmaceut. Biomed. 100, 357–364. https://doi.org/10.1016/j.jpba.2014.08.015.

Zhu, Y.X., et al., 2000. In vivo microdialysis and reverse phase ion pair liquid chromatography/tandem mass spectrometry for the determination and identification of acetylcholine and related compounds in rat brain. Rapid Commun. Mass Spectrom. 14, 1695–1700. https://doi.org/10.1002/1097-0231(20000930)14:18<1695::Aid-Rcm79>3.0.Co;2-5.